理學碩士 學位論文

염도 차 발전 적용을 위한 고농도 고분자전해질이 주입된 나노 채널 멤브레인

Densely charged polyelectrolyte-plugged nanochannel arrays for power generation from salinity differences

2016 年 2 月

서울大學校 大學院

化學部 分析化學專攻

郭 守 洪

Abstract

The efforts in many scientific fields for replacing fossil fuel-based energy generation have been continued to decline further climate changes. Recently, reverse electrodialysis (RED), one of the promising process for generating electrical power from salinity differences between the sea and river water, has drew keen attention as an alternative process for an electrical power production. RED is less vulnerable to external influences such as a weather and the alteration of day with night so that it is capable of producing stable the electrical power production. However, commercially available ion-exchange membranes (IEMs), fundamental elements in a RED system generating an electrical potential, have limitations in practical applications, e.g. high cost and short durability. Therefore, as the alternative, we developed polyelectrolyte-plugged IEMs supported by anodized aluminum oxide (AAO) arrays. The AAO array consist of well-distributed linear nanochannels but its low surface charge density leads to reduced ion-selectivity by thin electrical double layers (EDLs) formed on the inner wall of

nanochannels. When the AAO nanochannels were plugged with ion-selective polyelectrolytes, the polyelectrolytic AAO membrane (PAM) provided excellent ion selectivities and low area resistances.

Based on the salinity difference between sea and river water, the electric potential and area resistance of the PAMs were measured. The theoretical power densities calculated from the PAMs were comparable with those of commercially available IEMs. We also investigated the AAO frame influence on the PAM resistance by conducting comparative resistance measurements of a polyelectrolyte-plugged capillary. The results showed that the PAM resistance, for the higher power density, could be decreased by optimizing the AAO frame, e.g. expanding the porosity or reducing the membrane thickness.

Keyword: Reverse electrodialysis, Ion exchange membrane, Polyelectrolyte, Anodized aluminum oxide.

Student number: 2012-20265

Contents

1. Introduction

Electrical power generation from renewable energy resources, e.g. sun, wind, waves, and tidal power, has recently attracted much attention of scientists in opposition to environmental contamination that originates from burning fossil fuels worsen with increasing energy demands. Reverse electrodialysis (RED) is one of the promising processes generating electrical power from renewable energy resources. In the early 1950s, Pattle introduced the concept of electrical power generation exploiting permselective membrane in which cations or anions selectively diffuse from a concentrated solution, e.g. sea water, to a diluted one, e.g. river water, for the first time[1]. There are still critical issues for practical applications, for instance, high cost and short durability of membranes. In particular, biofouling seriously shortens the life time of membranes[2],[3]. Natural water contains a variety of substances that can cause mechanical damages to the membranes or block the charge transport pathways in the membranes.

Recently, functionalized nanochannel was suggested as a potential alternative to polymer-based ion-selective

membranes for energy harvesting devices[4],[5]. For the purpose of miniaturized power generators and micro batteries, nanofluidic channel may be more suitable structure compared to conventional organic membranes[6],[7] because inorganic nanochannels can provide more robust framework[8]. Surface-charged nanochannels counteract their charge imbalance by drawing counter-ions toward its surface while repelling co-ions in the opposite direction, forming electrical double layers (EDLs). Owing to the EDL overlap in nanochannel, counter-ions preferentially pass through the nanochannel from a concentrated solution to a diluted one. Such charge-selective transport of ions generates electrical potential gradient coming from the salinity differences. However, electrostatic functionalization on the inner wall of nanochannel has several limitations in terms of power generation. Manufacturing densely packed nanochannel arrays with linear and evenly distributed pores is an intricate process and only limited number of materials are available for fabrication of nanochannel arrays, e.g. anodized aluminum oxide (AAO)[9]-[11]. More importantly, ion selectivity substantially decreases when the nanochannels are

situated in a concentrated solution (e.g. sea water) because the EDL could become too thin to get overlapped[12]. To retain high ion-selectivity even in the condition of the concentrated electrolyte solution, surface charge commensurate with the electrolyte concentration is required, but it obviously has upper limit. Another way to do so is to reduce the diameter of channels to tens of nanometers or less[12],[13]. Nanochannel arrays with tens of nanometer scale is also a challenge to fabricate in terms of technology well as cost.

On the other hand, polyelectrolytes are the polymers that have electrostatic charges on the backbones of those. They are readily hydrated and show low resistivity, ion selectivity, and biocompatible properties when in the form of hydrogel. Harnessing these characteristics, novel iontronic devices such as diodes[14]-[16], transistors[17]-[19], and logic circuits[20],[21] were reported recently, suggesting information processor operating in aqueous media. Polyelectrolytes in aqueous solution, however, hardly exist stand-alone maintaining a given shape without framework. This property hinders practical applications of polyelectrolytes for functional devices and ion-

selective membranes with wide area. In this sense, we hypothesized that nanochannel array could serve as a framework physically supporting polyelectrolytes and limited ion-selectivity of nanochannel itself could be compensated by polyelectrolytes in it. Specifically, AAO offers rigid framework and polyelectrolyte in its nanochannels does high ion selectivity as well as conductivity. Here we report how polyelectrolyte can be stuffed in the nanochannels of a porous AAO array and how organic-inorganic hybrid materials as made work.

2. Experimental

2.1. Materials

All chemical reagents were purchased from Sigma-Aldrich Inc. if not indicated otherwise. Dialylldemethyl-ammonium chloride (DADMAC, 348279), 2-acrylamido-2-methyl-1-propanesulfonic acid (AMPSA, 282731), (3-aminopropyl)triethoxysilane (APTES, A3648), potassium persulfate (216224), 2-hydroxy-4'-(2-hydroxyethoxy)-2-methylpropiophenone (410896), *N,N'*-methylene-bisacryl-amide (146072) were used without further purification. AAO membranes (No. 6809-6022) were purchased from Whatman Ltd. 3-(trihydroxysilyl)-1-propanesulfonic acid (TPA, SIT8378.3) was from Gelest Inc.

2.2. Polyelectrolyte plugged AAO membrane manufacture

An AAO (200 nm in diameter and 60 μm in thickness) was used as a membrane framework. It was dipped in a solution of cationic or anionic monomer, DADMAC or AMPSA. Cation-selective polyelectrolytic AAO membrane (C-PAM) was prepared by the following process. Firstly, an AAO was immersed in dry acetone containing 5% (v/v) APTES for 1 h. After washing with 100 mL acetone, the AAO was placed on a hotplate at 120 ℃ at 20 min to ensure silanization. Using a syringe pump, an AMPSA monomer solution containing potassium persulfate and *N,N'*-methylene-bisacrylamide was pushed into the AAO channels. Then the AAO membrane was baked in an oven at 80 ℃ for 30 min. For preparation of an anion-selective polyelectrolytic AAO membrane (A-PAM), an AAO membrane was reacted with 1 mM TPA in ethanol for 30 min and washed with ethanol. Then the AAO membrane was baked at 70 ℃ overnight for the complete silanization. The arrays of silanized AAO membrane was filled with a DADMAC solution with 2-hydroxy-4'-(2-hydroxyethoxy)-2-

methylpro-piophenone and *N,N'*-methylene-bisacrylamide. Finally, the AAO membrane was exposed to the UV light (365 nm, 16 mW/cm) for 17.5 s for the photopolymerization. The manufactured PAMs were characterized by FESEM (Carl Zeiss, Germany) at the National Instrumentation Centre for Environmental Management of Seoul National University.

To investigate the density effect of the polyelectrolytes on the membrane properties, the PAMs were synthesized using various concentrations of monomers and cross-linkers (Table 1). The concentration ratio of the monomer to the cross-linker was fixed to maintain chemical structures of polyelectrolytes unchanged.

	AMPSA (M)	Cross-linker (mM)	Initiator (mM)
C-PAM100	2.81	7.54×10^{-2}	4.30×10^{-2}
C-PAM75	2.11	5.66×10^{-2}	4.30×10^{-2}
C-PAM50	1.41	3.77×10^{-2}	4.30×10^{-2}
C-PAM25	0.70	1.89×10^{-2}	4.30×10^{-2}
	DADMAC (M)	**Cross-linker (mM)**	**Initiator (mM)**
A-PAM100	4.20	6.76×10^{-2}	4.65×10^{-2}
A-PAM75	3.15	5.07×10^{-2}	4.65×10^{-2}
A-PAM50	2.10	3.38×10^{-2}	4.65×10^{-2}

Table 1. Recipe for the preparation of C-PAMs and A-PAMs.

2.3. Permselectivity measurement setup

Membrane potential was measured from the potential difference between a pair of Ag/AgCl reference electrodes that were in two compartments divided by the membrane of interest (Fig. 2-1). A potentiostat (CHI660a, CH Instrument) read an open circuit potential (OCP) from two reference electrodes immersed in 0.017 M and 0.510 M NaCl solutions. The volume of reservoirs was 10 mL and the diameter of membrane was 2 cm. OCP was measured once the membrane potential reached equilibrium.

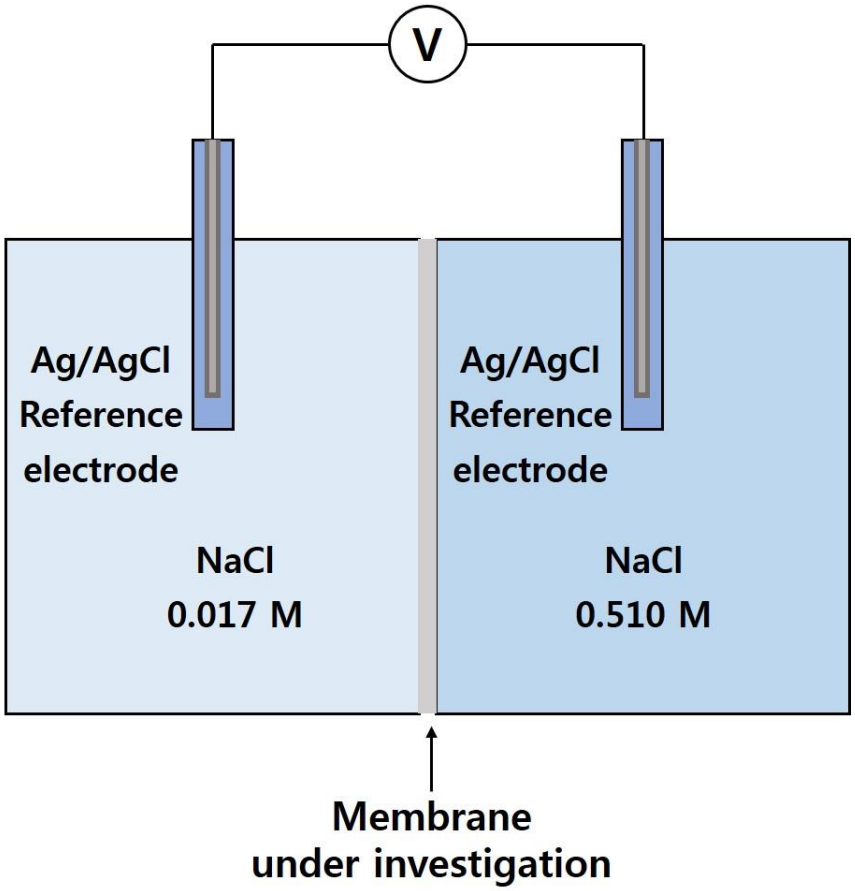

Figure 2-1. Scheme of experimental setting to measure perm-selectivity of ion exchange membrane.

2.4. Area resistance measurement setup

Area resistance of a membrane was determined by electrochemical impedance spectroscopy (Fig. 2-2). Applying sinusoidal modulation of 0.3 mA at a frequency of 1 kHz to the pair of Ag/AgCl planar electrode (1 cm^2), a galvanostat (Gamry reference600, Gamry instrument) read potential difference between two Ag/AgCl reference electrodes dipped in each compartment filled with 20 mL of 0.5 M NaCl solution. The potential drop across the membrane gave the information about the membrane impedance.

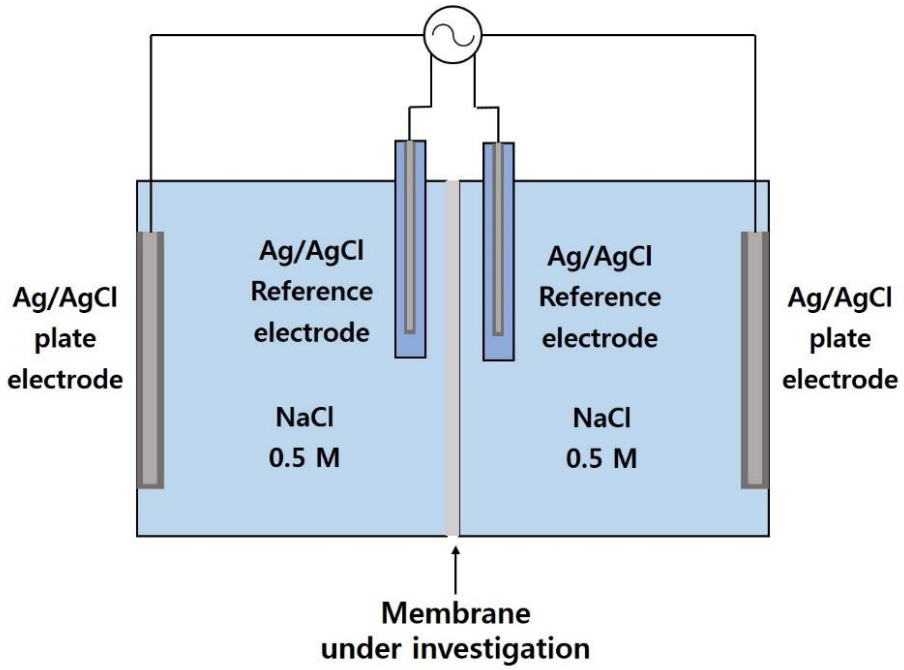

Figure 2-2. Scheme of experimental setting to measure area resistance of ion exchange membrane.

2.5. Resistivity of polyelectrolyte plugged capillary measurement setup

A capillary filled with polyelectrolytes was 5 cm long and 0.8 mm in diameter. The polymerization process was the same as that for PAM fabrication. Resistivity of polyelectrolytes was measured using electrochemical impedance spectroscopy (Fig. 2-3). The experimental parameters of the electrochemical impedance spectroscopy (EIS) were the same as for the measurement of the membrane area resistance. The capillary was connected the two reservoirs filled with 0.5 M NaCl solution.

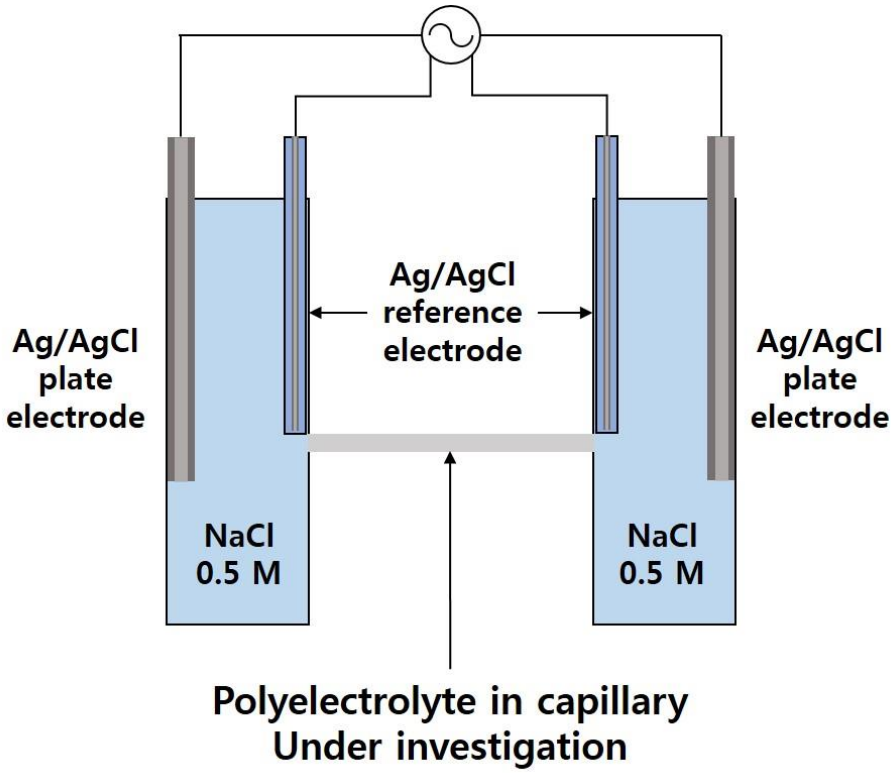

Figure 2-3. Scheme of experimental setup to measure the resistivity of polyelectrolyte in capillary. The capillary is 5 cm long and the cross section area of the polyelectrolyte phase interfaced with the solution is 0.8 mm in diameter.

3. Results and discussion

3.1. Silanized AAO surface identification with XPS

We silanized the AAO surface to functionalize its nanochannel arrays (~200 nm in diameter and 60 m in length). For the preparation of cation-selective polyelectrolytic AAO membrane (C-PAM), APTES was used to make the surface positively charged so that AMPSA monomers should be attracted as counter ions into AAO channels. Similarly, we introduced TPA to the AAO surface to get DADMAC monomers into the channels for preparation of anion-selective PAM (A-PAM).

The silanization results on the AAO channel surface were confirmed by X-ray photoelectron spectroscopy (XPS) (Fig 3-1, 3-2). The N1s XPS spectrum of the APTES-modified AAO resulted from overlapping of two peaks; NH_2 at 398.8 eV and NH_3^+ at 400.8 eV (Fig. 3-1b)[22]-[24]. In contrast, the bare AAO surface presented a broadened weak peak near 399 eV (Fig. 3-1a). It indicates the successful modification of the surface with APTES as intended. We also verified TPA functionalization on the AAO surface as evidenced by 2 species of SO_2^- (167.5 eV

for S2p3/2 and 168.6 eV for S2p1/2) and SO_3^- (169.1 eV for S2p3/2 and 170.3 eV for S2p1/2) from TPA-modified AAO (Fig. 3-2)[25],[26].

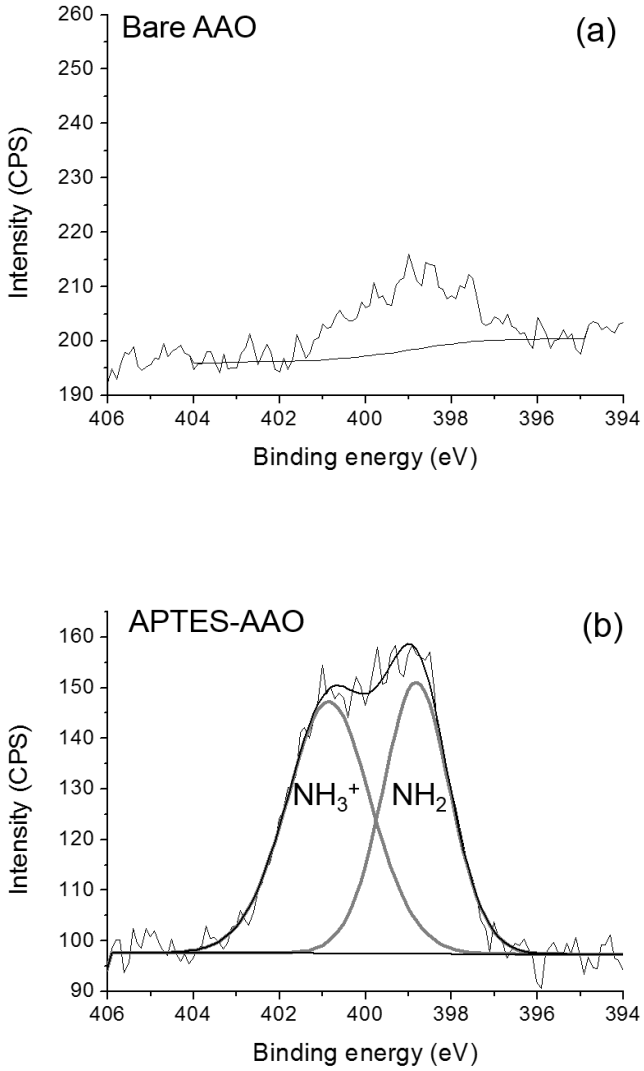

Figure 3-1. XPS spectra of N1s peak on the bare surface of AAO (a), APTES silanized AAO surface (b).

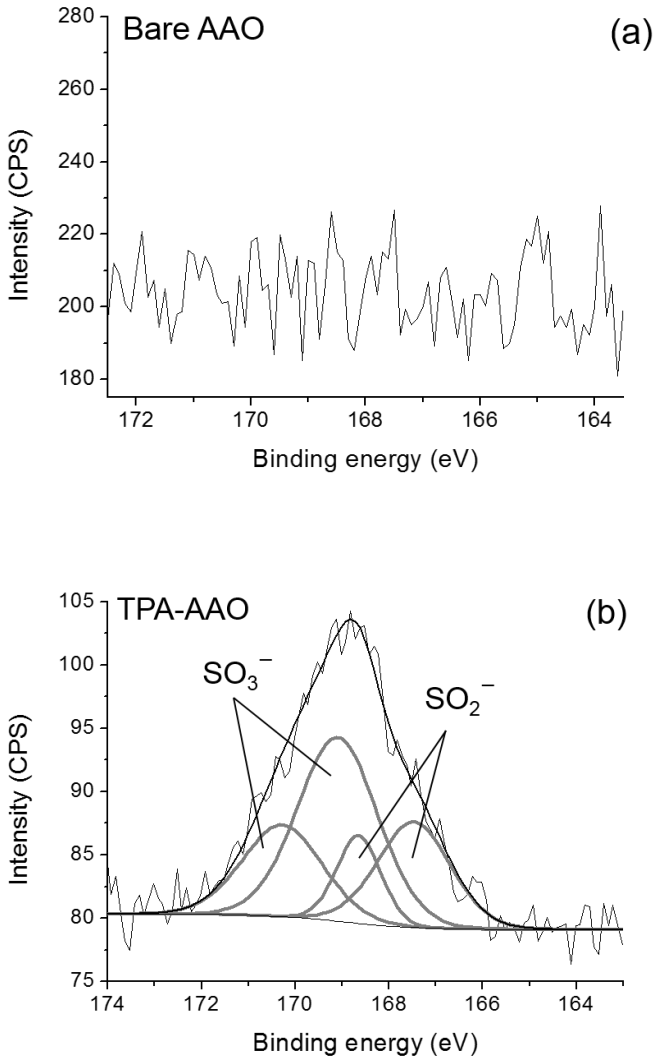

Figure 3-2. XPS Spectra of S2p on the bare surface of AAO (a), TPA silanized AAO surface (b).

3.2. Polyelectrolyte in AAO identification

3.2.1. SEM images

After the polymerization at the AAO support, we probed the polyelectrolytes created in the AAO channel by scanning electron microscopy (SEM). The cross section of the bare AAO surface showed linear, empty, and uniform pore arrays (Fig. 3-3a). As a consequence of the polymerization, all AAO arrays are filled with the polyelectrolytes (Fig. 3-3b and 3-3c).

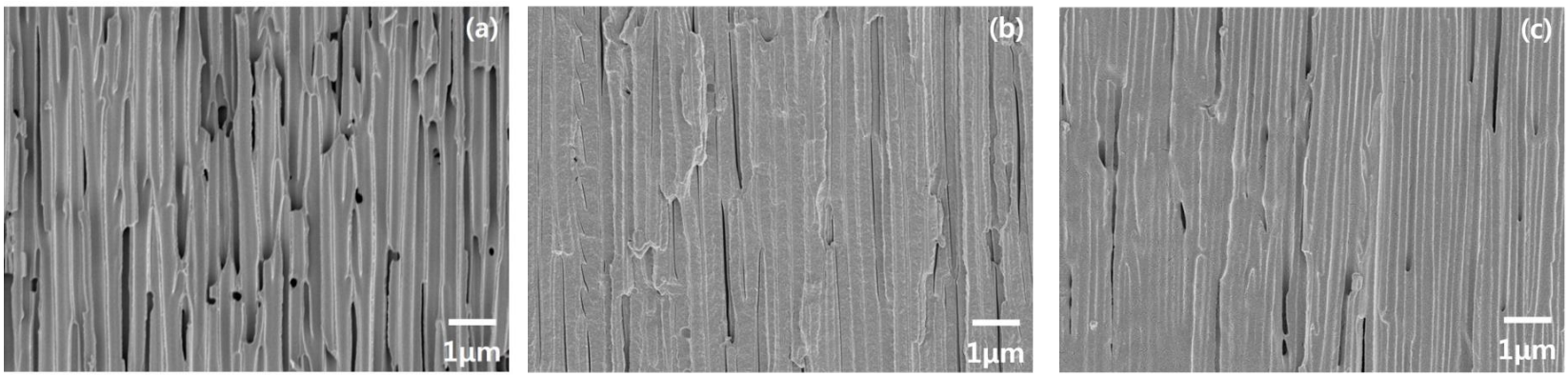

Figure 3-3. Scanning electron microscopy (SEM) images of cross sectional area of bare AAO (a), C-PAM (b) and A-PAM (c).

3.2.2. ATR-FTIR analysis

We compared the PAMs with the bare AAO surface as a control by means of ATR-FTIR. The C-PAM exhibited the characteristic peaks of polyAMPSA at 1642, 1183, and 1041 cm^{-1}, representing C=O stretching, asymmetric SO_3^-, and symmetric SO_3^- stretching vibrations, respectively (Fig. 3-4a)[27],[28]. The A-PAM also showed a strong peak at 1474 cm^{-1} which is the fundamental frequency for CH_3 bending vibrations of polyDADMAC whereas the bare AAO arrays showed no discrete peaks in the spectra (Fig. 3-4b)[29]. Consequently, the AAO arrays were full of organic polyelectrolytes, yielding organic-inorganic hybrid membranes with linear nanochannels that serve as a mechanical skeleton and minimize the resistance for ion transport.

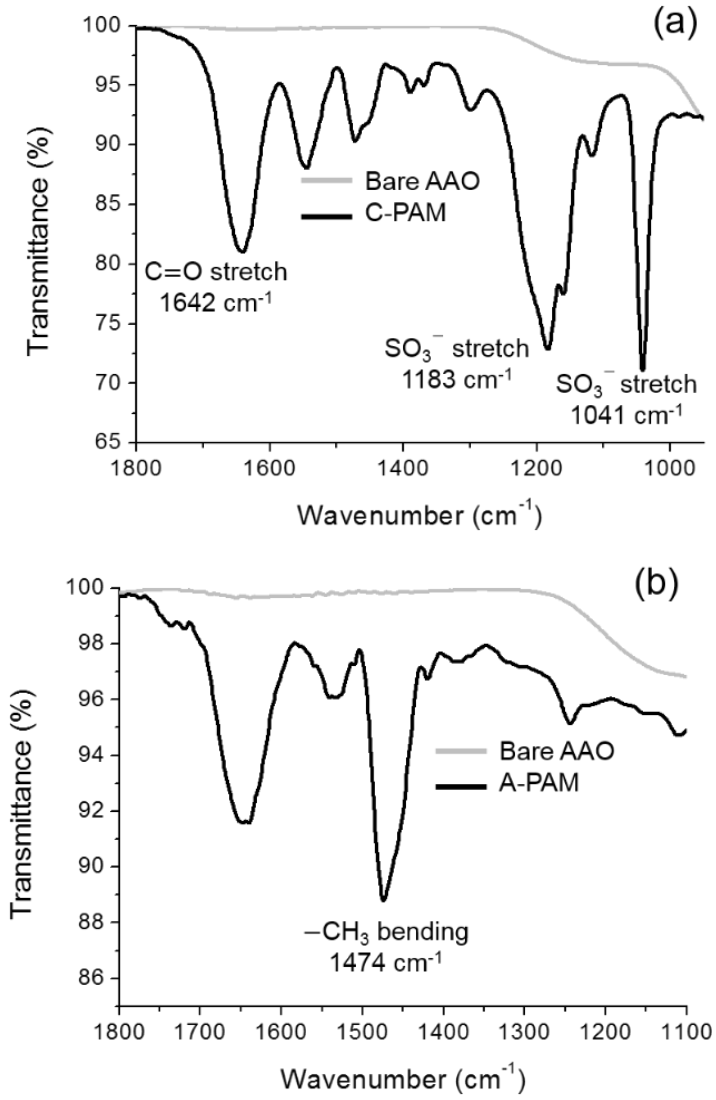

Figure 3-4. ATR-FTIR spectra of polyDADMAC-filled AAO membrane (a) and polyAMPSA-filled AAO membrane (b). Solid line and gray line indicate polyelectrolyte-filled AAO and bare AAO respectively.

3.3. Membrane characteristics evaluation

3.3.1. Permselectivity

We evaluated fundamental electrochemical characteristics of the PAMs as ion-exchange membranes. Permselectivity can be calculated from the electrical potential difference that is developed across a membrane:

$$E = \alpha \frac{RT}{nF} \ln \frac{\gamma_H C_H}{\gamma_L C_L} \quad (1)$$

where E is the electrical potential of the membrane, α is the permselectivity, n is the valence, R is the gas constant, T is the temperature, and γ is the mean activity coefficient of NaCl solution (0.686 for 0.51 M and 0.878 for 0.017 M NaCl solution)[30]. C_H and C_L represent high and low molar concentrations.

We fabricated a series of C-PAMs and A-PAMs varying the concentration of monomers and cross-linkers to investigate the membrane characteristics and optimize the conditions for membrane preparation. The concentration of monomers and

cross-linkers increased from C-PAM25 and A-PAM50 to C-PAM100 and A-PAM100 (Table 1). It should be noted that we excluded the irreproducible data of A-PAM25 because the concentrations of the monomer and the cross-linker were too low to be polymerized. Additionally, for the case of A-PAM50, several polymer fragments and unoccupied spaces with polyelectrolytes were observed along the nanochannels, indicating that the concentrations of the monomer and the cross-linker were still insufficient to stuff whole nanochannels with the polyelectrolytes after the polymerization (Fig. 3-5). As expected, the permselectivity of the PAMs gradually increased in proportion to the monomer concentration (Fig. 3-6) owing to increasing density of electrostatic charge. When the concentration of monomers and cross-linkers was almost saturated in the solution, C-PAM100 and A-PAM100 reached the highest permselectivities out of the PAMs tested (C-PAM100 99% and A-PAM100 89%). Therefore, we confirmed that the polyelectrolyte-filled AAO membranes provided excellent permselectivities which were not obtainable using

only bare AAO membranes (4.4% permselectivity as an AEM based on our experimental data).

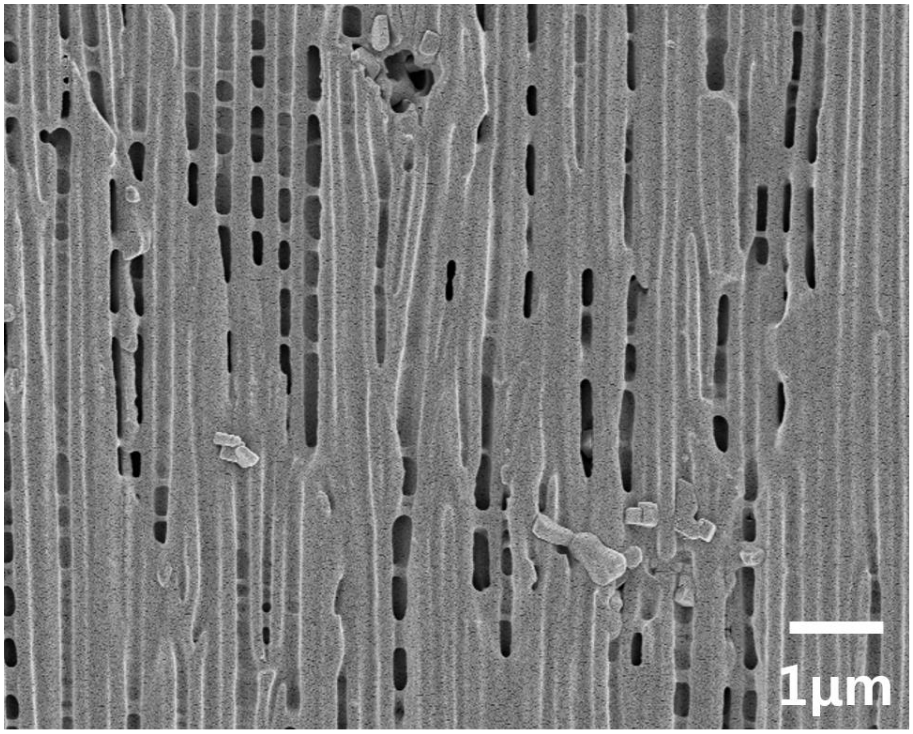

Figure 3-5. An image of scanning electron microscopy showing a cross sectional area of A-PAM50.

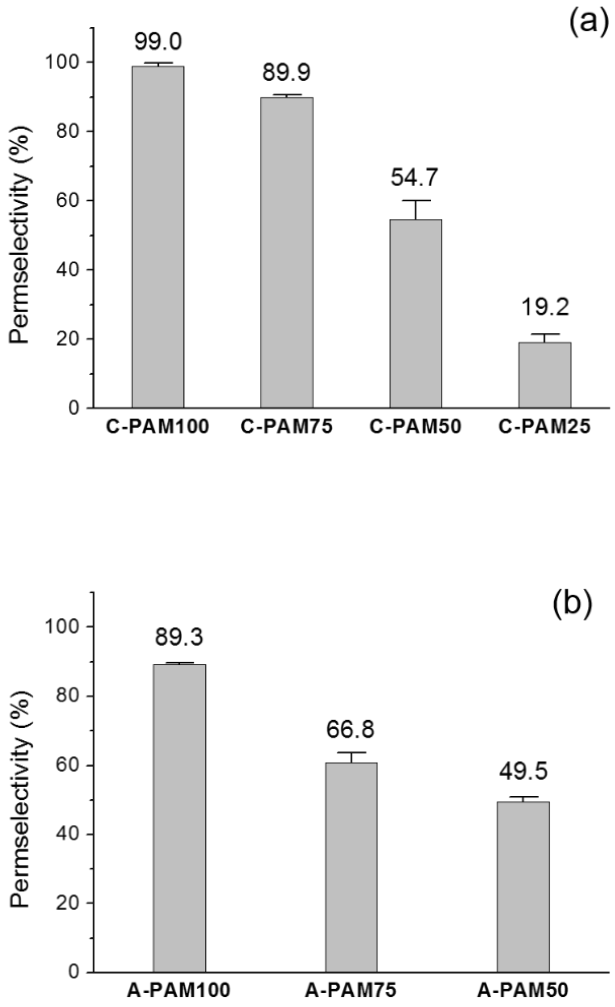

Figure 3-6. Permselectivities of the C-PAMs (a) and the A-PAMs (b). The error bars represent the standard deviations obtained from three independent measurements.

3.3.2. Area resistance

Electrochemical impedance spectroscopy (EIS) offers the information about the area resistance of the membranes. EIS has been widely used to investigate the electrochemical properties of ion-exchange membranes because it enables to extract individual components from the apparent total impedance, unlike direct current (DC) method[31]. The impedance of a membrane system comes from diffusion boundary layer (DBL), EDL, membrane itself, and solution (Fig. 3-7). We selectively obtained the resistances of the membrane and solution (R_{M+S}) by applying a sinusoidal modulation of 0.3 mA at a frequency of 1 kHz. At such a high frequency, impedances of EDL and the DBL can be assumed to be negligible because of their capacitance in parallel. Since the solution resistance (R_S) was measured in the absence of the membrane under the same experimental condition, we were able to calculate the pure membrane resistance (R_M) by subtracting R_S from the R_{M+S}.

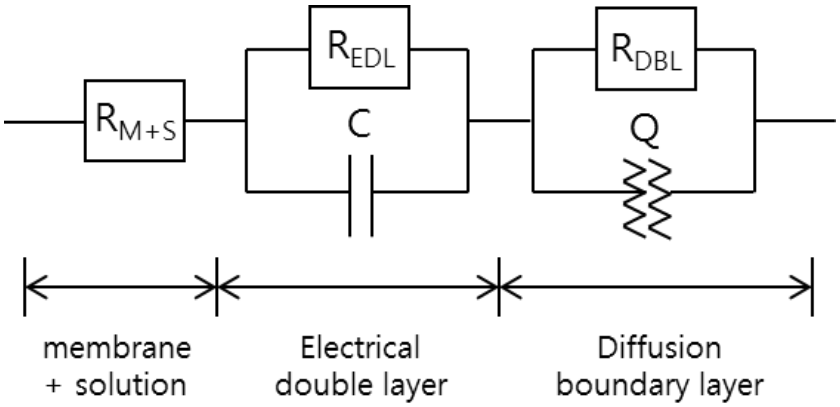

Figure 3-7. Total impedance of ion-exchange membrane. R_{M+S} is the sum of membrane and solution resistance and R_{EDL} is the resistance of the counter-ion transfers from the solution to the membrane through the EDL. C is the capacitance of the ionic charge at the EDL and R_{DBL} is the resistance of diffusion boundary layer. Q is the constant phase element representing non-ideal capacitance of the DBL.

Similar to the results of the permselectivity, the area resistance of the membranes was proportional to the concentration of monomers and cross-linkers (Fig. 3-8). Higher density of the polyelectrolyte leads to better permselectivity due to more electrostatic charge within given volume of the polymer network. However, the ion penetration through the AAO nanochannel is impeded by the densely packed polymer structures. Slower ion penetration means higher membrane resistance, resulting in lower ion current density. The area resistances of the A-PAMs were lower than the C-PAMs (Fig. 3-8) while the permselectivities of the C-PAMs were higher than the A-PAMs (Fig. 3-6). There should be a tradeoff between the membrane permselectivity and the area resistance.

Therefore, the concentration of the monomers and the cross-linkers should be optimized to obtain the best membrane for maximum electrical power density.

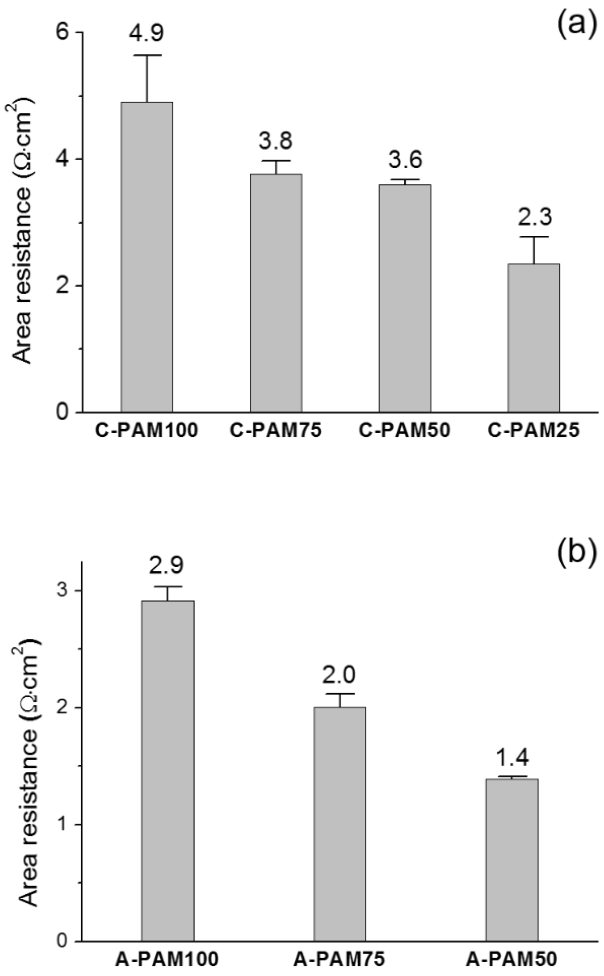

Figure 3-8. Area resistance of the C-PAMs (a) and the A-PAMs (b). The error bars indicate the standard deviations of three independent measurements.

Resistivity of polyelectrolytes in a capillary was measured for the comparison study with that of PAMs (Fig. 3-9). All conditions for polymerization were the same except the pores in which it occurred. The resistivity of C-PAM100 was about 110-fold higher than that of the polyAMPSA in the capillary (the polyAMPSA in the capillary 7.27 Ω·cm and the C-PAM100 817 Ω·cm). In the case of A-PAM100, the resistivity was about 8-fold higher than that of the polyDADMAC in the capillary (the polyDADMAC in the capillary 69.3 Ω·cm and the A-PAM100 543 Ω·cm). Interestingly, resistivity of the capillary filled with polyelectrolytes, polyDADMAC, was about 9-fold higher than that of polyAMPSA. In contrast, AAO membrane polyDADMAC, A-PAM100, showed about 2-fold lower resistivity than that of polyAMPSA-filled AAO membrane, C-PAM100. In order to raise the power, there are a few detailed issues to address. There may be voids unfilled with the polyelectrolytes in the nanochannels where ultra violet light does not reach during the photopolymerization. Minimizing the voids by sophisticatedly adjusting the experimental conditions would lead to reliable performance as well as higher power.

Porosity and length of the nanochannels of AAO framework are another parameters that need to be tuned further. Permselectivity and resistivity sensitively reflect the quality of the polyelectrolytes-AAO hybrid membranes so that the experiments shown in this work could provide canonical protocol and setup for optimization of organic charge-selective stuff in inorganic channel framework.

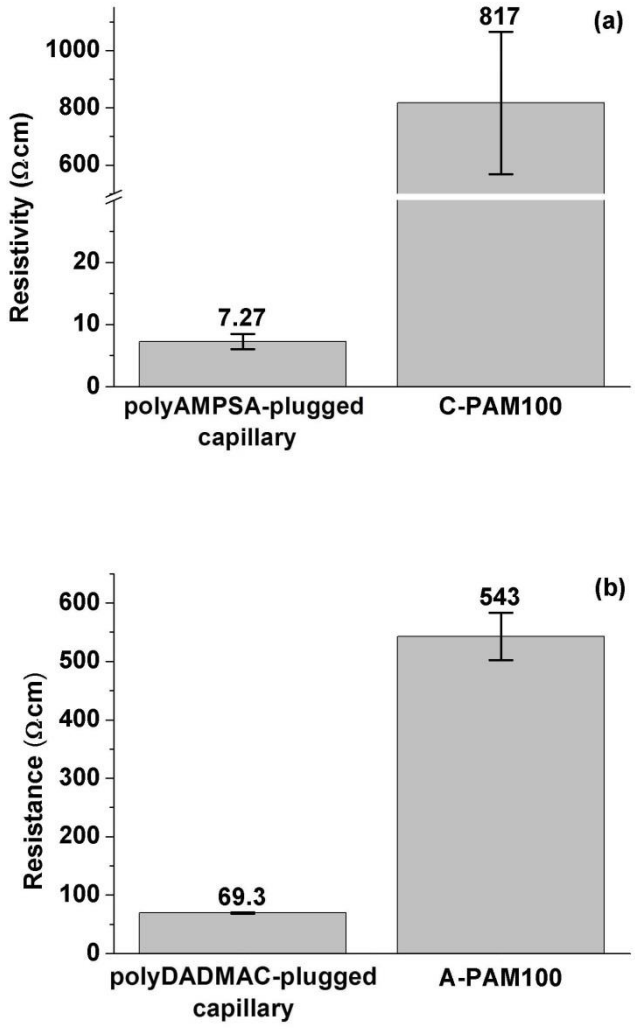

Figure 3-9. Resistivity comparison between the polyelectrolyte-plugged capillary and the PAM100s; (a) C-PAM100 and (b) A-PAM100.

3.4. Theoretical power density expectation

We finally estimated theoretical power densities based on the data of the permselectivities and the area resistances that were measured. Recently, P. Długołęcki et al. calculated the theoretical power output using a range of properties of commercially available membranes and achieved the fair comparison between the membranes under equal conditions[32]. The theoretical power output was calculated by Equation (2):

$$W_{\max} = NA\frac{[\alpha_{av}\frac{RT}{F}ln\left(\frac{a_c}{a_d}\right)]^2}{R_{AEM}+R_{CEM}+\left(\frac{d_c}{\kappa_c}\right)+(\frac{d_d}{\kappa_d})} \qquad (2)$$

where N is the number of membrane pairs, A is the area of membrane, α_{av} is the average permselectivity , R_{AEM} is the anion exchange membrane resistance, R_{CEM} is the cation exchange membrane resistance, d is the thickness of solution channel, and κ is the conductivity. a_c and a_d stand for the activities for the concentrated and diluted solution, respectively. We supposed that d_c and d_d are 150 μm and κ_d and κ_c are 0.192 and

4.684 S/m, respectively. Equation (2) includes the membrane potential and the resistances of the membranes and the solutions, while excluding necessary pumping energy for water supplies, resistances of concentration polarization, and shadow effects caused by spacers[33]. For a CEM membrane, α_{av} is replaced by the CEM permselectivity ignoring the AEM resistance. The solution channel thickness is divided by two.

Based on the permselectivities and the area resistances recorded, we calculated theoretical power densities of RED systems consisting of the proposed polyelectrolyte-AAO hybrid membranes (Fig. 3-10). The theoretical power densities of the C-PAM100 and the A-PAM100 were 3.5 W/m^2, comparable to commercially available membranes[32]. In addition, when compared with bare AAO membranes as AEMs, based on the obtained experimental data, the PAMs showed much higher power density than the bare AAO membrane (0.011 W/m^2 calculated from 1.34 Ω·cm^2 area resistance and 4.4% permselectivity).

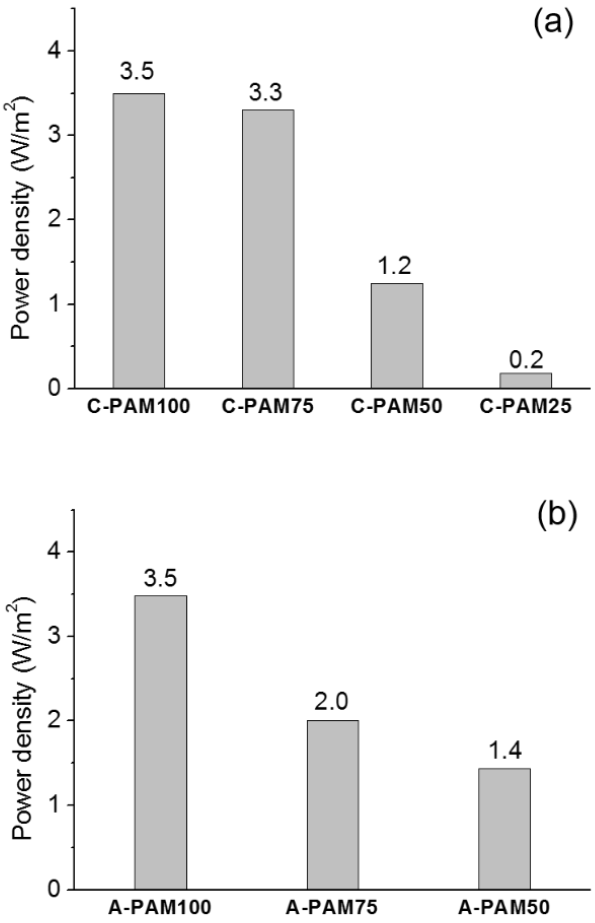

Figure 3-10. Estimated theoretical power densities of the C-PAMs (a) and the A-CAMs (b). The theoretical power densities were calculated from the average of the permselectivities and the resistances from Fig. 3-6 and Fig. 3-8, respectively.

4. Conclusion

We have successfully developed the organic ion-selective polyelectrolytes supported by the inorganic frameworks of AAO for the application of RED. The PAMs exhibited excellent permselectivities and low area resistances comparable to the commercially available ion-exchange membranes. The density of the polyelectrolytes in the PAMs was found to strongly affect the membrane characteristics that are closely linked to the electrical power production, especially for the RED application. We investigated the effects of the AAO framework on the membrane resistance. The results indicate that the combined system of charge-selective organic material filled in inorganic nanochannel framework has great potential for further advance in functional ion transport. For instance, the tendency found in the data strongly imply that the area resistance of the PAMs could be improved by adjusting the geometric features of AAO arrays, e.g. widening pore spaces or reducing membrane thickness. In spite of its intuitive structural interest inspiring futuristic engineering, intrinsically AAO itself is mechanically brittle, which one of the serious obstacles for practical

applications. By integrating with organic polymers, its physical weakness is expected to be relieved, at least maintained, acting as a framework. The ion-selective PAMs in this work suggest a new strategy for portable energy harvesting devices where the concentration gradients present. Miniaturized power supply systems such as micro batteries to operate biosensors for the point-of-care system is another possible targets that may be benefited by the ion-selective PAMs.

5. References

[1] Pattle, R. *Nature* 1954, *174*, 660.

[2] Post, J. W., Hamelers, H. V. M. & Buisman, C. J. N. *Journal of Membrane Science* 2009, *330*, 65-72.

[3] Vermaas, D. A., Kunteng, D., Saakes, M. & Nijmeijer, K. *Water Research* 2013, *47*, 1289-1298.

[4] Choi, E., Kwon, K., Kim, D. & Park, J. *Lab on a Chip* 2015, *15*, 168-178.

[5] Kim, D.-K., Duan, C., Chen, Y.-F. & Majumdar, A. *Microfluidics and nanofluidics* 2010, *9*, 1215-1224.

[6] *Lab on a Chip* 2010, *7*, 1234-1237.

[7] Wang, W. et al. *Nano letters* 2012, *12*, 655-660.

[8] Chu, K.-L., Shannon, M. A. & Masel, R. I. *Journal of the Electrochemical Society* 2006, *153*, A1562-A1567.

[9] Liu, N.-W. et al. *Advanced Materials* 2005, *17*, 222-225.

[10] Asoh, H. et al. *Journal of Vacuum Science & Technology B* 2001, *19*, 569-572.

[11] Masuda, H. et al. *Applied Physics Letters* 1997, *71*, 2770-2772.

[12] Boo, H. et al. *Journal of the American Chemical Society* 2004, *126*, 4524-4525.

[13] Cheng, L.-J. & Guo, L. J. *Nano letters* 2007, *7*, 3165-3171.

[14] Han, J. H. et al. *Small* 2011, *7*, 2629-2639.

[15] Fang, J. et al. *Journal of the American Chemical Society* 2010, *133*, 683-685.

[16] Cayre, O. J., Chang, S. T. & Velev, O. D. *Journal of the American Chemical Society* 2007, *129*, 10801-10806.

[17] Seo, J. H. et al. *Journal of the American Chemical Society* 2009, *131*, 18220-18221.

[18] Herlogsson, L. et al. *Advanced Materials* 2008, *20*, 4708-4713.

[19] Lee, S. W. et al. *Nano letters* 2009, *10*, 347-351.

[20] Han, J. H., Kim, K. B., Kim, H. C. & Chung, T. D. *Angewandte Chemie* 2009, *121*, 3888-3891.

[21] Chun, H. G. & Chung, T. D. in *Annual Review of Analytical Chemistry*, *Vol 8* Vol. 8 *Annual Review of Analytical Chemistry* (eds R. G. Cooks & J. E. Pemberton) 2015, 441-462.

[22] Acres, R. G. et al. *The Journal of Physical Chemistry C* 2015, *116*, 6289-6297.

[23] Jani, A. M. M. et al. in *Smart Materials, Nano-and Micro-Smart Systems.* 72670T-72670T-72610 (International Society for Optics and Photonics).

[24] Martin, H. J., Schulz, K. H., Bumgardner, J. D. & Walters, K. B. *Langmuir* 2007, *23*, 6645-6651.

[25] Nasef, M. M. & Saidi, H. *Applied surface science* 2006, *252*, 3073-3084.

[26] Nasef, M. M., Saidi, H., Nor, H. M. & Yarmo, M. A. *Journal of applied polymer science* 2000, *76*, 336-349.

[27] Xu, G., Gao, S., Ji, X. & Zhang, X. *Soft Nanoscience Letters* 2014 *2014*.

[28] Rastogi, P. K., Krishnamoorthi, S. & Ganesan, V. *Journal of Applied Polymer Science* 2012, *123*, 929-935.

[29] Bhalerao, U. M., Acharya, J., Halve, A. K. & Kaushik, M. P. *RSC Advances* 2014, *4*, 4970-4977.

[30] Dlugolecki, P. E. 2009, University of Twente.

[31] Park, J. S., Choi, J. H., Woo, J. J. & Moon, S. H. *Journal of Colloid and Interface Science* 2006, *300*, 655-662.

[32] Dlugolecki, P., Nymeijer, K., Metz, S. & Wessling, M. *Journal of Membrane Science* 2008, *319*, 214-222.

[33] Długołęcki, P., Gambier, A., Nijmeijer, K. & Wessling, M. *Environmental science & technology* 2009, *43*, 6888-6894.

국문 초록 (Abstract in Korean)

화석연료를 대체할 재생 에너지 개발에 대한 노력은 이제 인류 전반의 화두가 되고 있다. 특히 해수와 담수의 염분 농도 차를 이용한 발전 방법 중의 하나인 역전기투석 발전은 다른 방법에 비해 지역적 한계를 제외한 외부의 영향을 적게 받아 지속적인 에너지 발전이 가능하다는 장점을 지녀 많은 관심을 받고 있으나, 소모성 부품인 이온교환막의 높은 가격과 짧은 교환 주기가 단점으로 지적 받고 있다. 이에 기존 폴리머 기반 이온교환막의 대안으로서, 나노다공성 산화알루미늄에 전하 밀도가 높은 고분자전해질을 채워 넣은 이온교환막을 개발하였다. 고분자전해질이 채워진 산화알루미늄 이온교환막은 고분자전해질의 종류에 따라 양전하 혹은 음전하를 띠어 역전기투석 발전에 필요한 이온교환막 쌍을 만드는 데 유용하다. 또한 높은 전하밀도를 갖고 있으나 강도가 낮아 막 형태를 유지할 수 없다는 고분자전해질의 성질과, 직선형태의 고른 나노 채널을 가지지만 이온교환막 역할을 하기에는 다소 부족한 전하 밀집도를 갖는 나노다공성 산화알루미늄의 장단점이 적절히 조화된 특징을 가지고 있다.

해수와 담수의 실제 염분 농도에 기반하여 단일 이온교환막이 발생시키는 전위와 단위 면적 당 저항을 측정하였고, 이를 토대로 계산한 이론 상 발생 가능 전력 밀도는 폴리머 기반 이온교환막과

대등한 정도를 보였다. 또한, 고분자전해질이 채워진 모세관의 비저항과 이온교환막의 비저항을 비교하여 산화알루미늄의 개선을 통해 더욱 높은 전력 밀도를 이끌어낼 수 있음을 확인하였다.

주요어 : 역전기투석 발전, 이온교환막, 고분자전해질, 나노다공성 산화알루미늄

학번 : 2012-20265